Cancer Gene Therapy (2006) 13, 606–618

www.nature.com/cgt

ORIGINAL ARTICLE

Employment of liver tissue slice analysis to assay hepatotoxicity linked to replicative and nonreplicative adenoviral agents

MA Stoff-Khalili[1,2], AA Rivera[1], LP Le[1], A Stoff[1,3], M Everts[1], JL Contreras[1], D Chen[4,5], L Teng[5], MG Rots[6], HJ Haisma[6], RP Rocconi[1], GJ Bauerschmitz[2], DT Rein[2], M Yamamoto[1], GP Siegal[1], P Dall[2], J Michael Mathis[7] and DT Curiel[1]

[1]*Division of Human Gene Therapy, Departments of Medicine, Obstetrics, Pathology, Cellular Biology, Surgery and the Gene Therapy Center, University of Alabama at Birmingham, Birmingham, AL, USA;* [2]*Department of Obstetrics and Gynecology, University of Duesseldorf, Medical Center, Duesseldorf, Germany;* [3]*Department of Plastic and Reconstructive Surgery, Dreifaltigkeits-Hospital, Wesseling, Germany;* [4]*Biostatistics and Bioinformatics Unit, Comprehensive Cancer Center, UAB, Birmingham, AL, USA;* [5]*Microarray Shared Facility, Comprehensive Cancer Center, UAB, Birmingham, AL, USA;* [6]*Department of Therapeutic Gene Modulation, Groningen University, Institute for Drug Exploration, Groningen, the Netherlands; and* [7]*Department of Cellular Biology and Anatomy, Louisiana State University Health Sciences Center, Shreveport, LA, USA*

Whereas virotherapy has emerged as a novel and promising approach for neoplastic diseases, appropriate model systems have hampered preclinical evaluation of candidate conditionally replicative adenovirus agents (CRAds) with respect to liver toxicity. This is due to the inability of human viral agents to cross species. We have recently shown the human liver tissue slice model to be a facile means to validate adenoviral replication. On this basis, we sought to determine whether our *ex vivo* liver tissue slice model could be used to assess CRAd-mediated liver toxicity. We analyzed and compared the toxicity of a conditionally replicative adenovirus (AdΔ24) to that of a replication incompetent adenovirus (Adnull [E1−]) in mouse and human liver tissue slices. To accomplish this, we examined the hepatic apoptosis expression profile by DNA microarray analyses, and compared these results to extracellular release of aminotransferase enzymes, along with direct evidence of apoptosis by caspase-3 immunhistochemical staining and TUNEL assays. Human and mouse liver tissue slices demonstrated a marked increase in extracellular release of aminotransferase enzymes on infection with AdΔ24 compared to Adnull. AdΔ24-mediated liver toxicity was further demonstrated by apoptosis induction, as detected by caspase-3 immunohistochemical staining, TUNEL assay and microarray analysis. In conclusion, concordance of CRAd-mediated apoptosis in both the human and the mouse liver tissue slice models was demonstrated, despite the limited replication ability of CRAds in mouse liver slices. The results of this study, defining the CRAd-mediated apoptosis gene expression profiles in human and mouse liver, may lay a foundation for preclinical liver toxicity analysis of CRAd agents.

Cancer Gene Therapy (2006) **13,** 606–618. doi:10.1038/sj.cgt.7700934; published online 6 January 2006

Keywords: hepatotoxicity; liver; tissue slice; adenovirus; CRAd; apoptosis; microarray

Introduction

Conditionally replicative adenoviruses (CRAds) have shown significant antitumor efficacy in animal models and are currently being evaluated as oncolytic agents for cancer therapy in a number of clinical trials.[1,2] Clinical toxicity of adenovirus is primarily hepatic, based on the tropism of the virus to the liver.[3,4] The adenoviral-mediated liver toxicity involves both an acute innate response[5] as well as adenovirus sequestration followed by hepatotoxicity as shown with an increase in serum transaminases and diagnostic histopathology.[6] Thus, the practical realization of successful clinical trials is the development of a tumor-selective adenovirus, which replicates in the tumor but not in normal liver.

While the acute innate response to adenoviral infection in the liver has been characterized,[5,7] the evaluation of direct hepatotoxicity by adenoviruses in a virotherapeutical context has been limited. This is mainly due to limited available model systems for preclinical evaluation of viral-mediated liver toxicity. For a variety of reasons

Correspondence: Dr DT Curiel, Division of Human Gene Therapy, Gene Therapy Center, University of Alabama at Birmingham, 901 19th Street South, BMR2 502, Birmingham, AL 35294-2172, USA. E-mail: curiel@uab.edu
Received 17 August 2005; revised 20 October 2005; accepted 15 November 2005; published online 6 January 2006

mice have been employed as the prototypic animal model for preclinical study of virotherapy agents. Ideally, a mouse model should mimic the target human disease in its etiology, genetics, clinical presentation, and progression.[8] However, this approach has been challenging in the field of virotherapy because human adenoviruses can presumably only partially replicate in rodents.[9,10] Thus, the development of stringent substrate systems to allow the fullest preclinical characterization of CRAd-mediated direct hepatotoxicity is a central task in the field of virotherapy.

To address this issue, we endeavored to explore the utility of precision-cut slices derived from human or murine livers as a tool to characterize *ex vivo* liver toxicity mediated by CRAds in a preclinical context. Precision-cut tissue slice technology offers a powerful and representative *ex vivo* model system for preclinical infectivity analysis, as the human liver tissue slices contain all the cell types present in whole liver and maintain their three-dimensional structure *in vitro*.[11–13] We have recently explored this method to provide a facile means to ascertain the replicative specificity of CRAd agents in a stringent context that parallels human clinical use. Of note, gene expression profiles in liver tissue slices have been shown to be similar to the *in vivo* gene expression in a variety of study contexts[11] and, thus, represents the most stringent available *ex vivo* model for human liver.[14]

Based on the available studies of adenovirus-mediated hepatotoxicity,[6] we hypothesized that apoptosis of hepatocytes is a major mechanism involved in CRAd-mediated liver toxicity.[15,16] For this reason, we examined the genes involved in Ad-mediated apoptosis in human and liver tissue slices using DNA microarrays. Consistent with this concept, conservation between mouse and human genes in respect to apoptosis programs has been reported.[17]

In this study, we analyzed and compared the direct mediated toxicity of a replication competent adenovirus to that of a replication incompetent adenovirus in mouse and human liver tissue slices. We utilized AdΔ24, which contains a 24-bp deletion in the CR2 of the E1A gene,[18,19] as a representative CRAd to determine differences in liver toxicity compared to that of a nonreplicative adenovirus Adnull, which is E1-deleted. To accomplish this, we examined the apoptosis expression profile by DNA microarray analyses of adenovirus-infected liver tissue slices, and compared these results to extracellular release of aminotransferase enzymes, along with direct evidence of apoptosis by caspase-3 immunhistochemical staining and TUNEL assays. The results of this study, defining the similarities and differences in adenoviral induced apoptosis in our *ex vivo* model using human and mouse liver slices may lay a foundation for preclinical liver toxicity analysis of CRAd agents.

Materials and methods

Human primary liver tissue samples

Approval was obtained from the Institutional Review Board for all studies on human tissue. Human liver samples were obtained (Department of Surgery, University of Alabama at Birmingham (UAB)) from eight adenovirus seronegative donor livers prior to transplantation into recipients. All liver samples were flushed with University of Wisconsin (UW) solution (ViaSpan, Barr Laboratories, Inc. Pomona, NY) before harvesting and kept on ice in UW solution until slicing. Time from harvest to slicing was kept at an absolute minimum (<2 h).

Mouse primary liver tissue samples

Ten C57BL/6 mice ranging in age from 6 to 10.5 weeks were used for this study after receipt of approval from the Institutional IACUC. Animals were killed by CO_2 asphyxiation, and liver samples were obtained. Time from harvest to slicing was kept at an absolute minimum (<2 h).

Slice preparation with the krumdieck tissue slicer

The Krumdieck tissue slicing system (Alabama Research & Development) was used in accordance with the manufacturer's instructions and previously published techniques.[12,20] An 8 mm coring device (Alabama Research and Development, Birmingham) was used to retrieve an 8 mm diameter core of tissue from the liver (human and mouse). This was then placed in a slicer filled with ice-cold culture media. Slice thickness was set at 250 μm using a tissue slice thickness gauge (Alabama Research and development) and slices were cut using a reciprocating blade at 30 r.p.m. Afterwards, these slices were stored in ice-cold culture media, which served as a wash/equlibration solution between preservation in UW solution and culture media.

Tissue slice culture

Tissue slices were placed into six-well plates (1 slice/well) containing 2 ml of complete culture media (William's Medium E with 1% antibiotics, 1% L-glutamine, and 10% FBS). The plates were then incubated at 37°C/5% CO_2 in a humidified environment for up to 48 h. A plate rocker set at 60 r.p.m. was used to agitate the slices and ensure adaequate oxygenation and viability.[13]

Viral infection

Adnull, an E1 deleted adenovirus, was chosen as a control nonreplicating virus. The CRAd AdΔ24 has been described previously (ref), and was constructed by homologous recombination in 'E1-complementing 293' cells between the pXC1 (Microbix Biosystems, Toronto, Canada) derivative PXC1-Δ24, carrying a 24-bp deletion in the pRb-binding CR2 domain of E1A,[18] and pBHG11. All viruses used in this study have no reporter gene. All viral infections were performed with 500 viral particles/cell in complete culture media containing 2% FBS. Cell number for tissue slices was estimated at 1×10^6 cells per slice based on a 10-cell thick slice ($\sim 250\,\mu$m) and 8-mm slice diameter. Infections were allowed to proceed for the intended time, subsequently media was removed and replaced with complete culture media containing 10%

FBS. Slices were removed from culture at 4, 10, 26 or 28 and 43 h postinfection.

RNA preparation

Tissue slices, both infected and noninfected (as a control), were placed in RLT buffer (RNEasy RNA extraction kit, Qiagen, Valencia, CA) with β-mercaptoethanol (Sigma, St Louis, MO). Slices were homogenized immediately with an ultrasonic sonicator (Fisher Scientific Model 100) at a setting of 15 W for 10 s. After centrifuging the homogenate, the supernatant was transferred to separate Eppendorf tubes for subsequent RNA purification with the Qiagen RNEasy kit, according to the manufacturer's directions. Purified RNA samples were eluted with 30 μl of DNAse/RNAse free water and stored at -80°C until analysis.

Assay of adenovirus copy number

Quantitative real-time RT-PCR was performed for the E4 region of adenovirus as previously described,[14,21] using the glyceraldehyde-3-phosphate dehydrogenase (GAPDH) human housekeeping gene expression as an internal control. Results are presented as E4 copies/ng of total RNA.

Direct liver toxicity analysis of Adnull and AdΔ24 by determination of liver enzymes levels

The levels of alanine transaminase (ALT), lactate dehydrogenase (LDH), and aspartate aminotransferase (AST) were determined in the culture media by the SFBC protocol.[13] We quantitated ALT, LDH, and AST levels at 4, 10, 28, and 43 h postinfection in human liver tissue slices from eight different patients (University of Alabama Hospital Laboratories, University of Alabama at Birmingham, AL) and 10 mice (ANIMALLABS, Diagnostic testing, George Carden, Birmingham, AL).

Microarray hybridization

For gene expression analysis, the commercially available Affymetrix Human Genome U133 Plus 2.0. Array and Mouse Genome 430 2.0 Array were used. The Human Genome U133 Plus 2.0 array contains over 47 000 transcipts including 38 500 well-known genes. The Mouse Genome 430 2.0 contains 39 000 transcripts including 34 000 well-characterized genes. A total of six expression arrays were analyzed, three Human Genome U133 Plus 2.0 arrays for human liver tissue slices (noninfected, Adnull- and AdΔ24-infected liver tissue-slices) and three Mouse Genome 430 2.0 arrays for mouse liver tissue slices (noninfected, Adnull- and AdΔ24-infected liver tissue slices). Detailed procedures for RNA labeling and array process are presented in the Manufacturer's Gene Chip Expression Technical Manual (Affymetrix). Briefly, total RNA in the amount of 2 μg of each sample was used for double-stranded cDNA generation by linear amplification using oligo dT-T7 primer and reverse transcriptase. Subsequently, biotin-labeled cRNA were synthesized by *in vitro* transcription (IVT) using the 3′-Amplification Reagents for IVT labeling (Affymetrix). The quality of total RNA and the quality of biotin-labeled cRNA were determined using the RNA Nano chip on Agilent BioAnalyzer. Prior to hybridizing to the expression arrays, the quality of the hybridization target was determined by hybridization to a Test 3 array that indicated the efficacy of the RT/IVT reaction by the ratios of expression level of 5′–3′ of house-keeping genes (β-actin and GAPDH). The arrays were hybridized overnight at 45°C for 16 h in a GeneArray Hybridization Oven 640 (Affymetrix). The next day, the arrays were washed and stained in the Fluidics Station 450 (Affymetrix) and scanned by the High Resolution GeneChip Scanner 3000 (Affymetrix). Gene expression levels were extracted using GeneChip Operating Software (GCOS 1.1, Affymetrix) and paired comparison between the gene expression levels in the Ad treatment groups and that in the untreated group were performed to determine the fold change for each transcript. The expression level and/or fold change were then subjected to data query and data mining in Data Mining Tool (DMT).

Microarray data analysis and annotation

We generated a list of genes involved in apoptosis (pro- or antiapoptotic), which were derived from an annotation file downloaded from the Affymetrix website (www.affymetrix. com). The list currently contains 725 probe sets equivalent to 314 genes. The microarray-derived probe set intensities were first filtered by fold changes and then by functions such as those pertaining to apoptosis. Given the exploratory nature of the microarray used in this study, the filtered list was later selectively verified by other methods such as RT-PCR.

To compare human vs mouse gene expression, the same genes (or probe set identifiers, IDs) from both human and mouse were matched based on an ortholog file downloaded from the Affymetrix web site. The file contains all probe sets IDs of human U133 plus chip and their matching mouse 430-2 chip probe set IDs. The file was used to generate lists of genes involved in apoptosis that contained genes common to both human and mouse liver tissue slices (155 genes) or genes unique to either human liver tissue slices (150 genes) or mouse liver tissue slices (90 genes).

Quantitative real-time reverse transcriptase PCR

To further validate the microarray results, quantitative real-time RT-PCR was performed. Fluorescent TaqMan probes and the primer pairs used for real-time RT-PCR were designed using Primer Express 1.0 (Perkin-Elmer, Foster City, CA) and synthesized by Applied Biosystems (Foster City, CA). Nine messenger RNAs (mRNAs) were analyzed, including EGLN3, BNIP3L, TIA1, CD38, GADD45B, BAX, BCL10, CASP3 and CASP4. GAPDH was used as an internal control. cDNA was prepared from total RNA samples using a first strand synthesis kit (Invitrogen), according to the manufacturer's protocol. For real-time RT-PCR assay, each 9 μl PCR reaction contained 3 mM $MgCl_2$, 300 μM each dATP, dCTP, and dGTP, 600 μM dUTP, 100 nM of forward, reverse primers, and probe, 1 U of r*Tth* DNA polymerase, 0.025% BSA, and RNase-free water. Plasmid standard or 1 μl of RNA

sample was added into each assay tube. Negative controls with no template were performed for each reaction series. Real-time PCR reaction was carried out using a LightCycler™ System (Roche Molecular Biochemicals, Indianapolis, IN). Thermal cycling conditions were subjected to 30 min at 48°C, 10 min at 95°C, then 40 cycles of 15 s at 95°C, and 1 min at 60°C. Data were analyzed with LightCycler software.

Assessment of apoptosis by TUNEL assay

Apoptosis was assessed by detection of DNA fragmentation using an *in situ* TUNEL assay and examined by light microscopy.

Caspase-3 staining

Formalin-fixed, paraffin-embedded human and mouse liver tissue slices were stained with a rabbit polyclonal antibody specific for caspase-3 (Cleaved Caspase-3 Ab, Cell Signaling Technology, # 9661). Biotinylated goat anti-rabbit antibody was added as the secondary bridging antibody to HRP-conjugated streptavidin. Staining was visualized with a DAB/$NiCl_2$ chromogen. As a negative control, staining was performed without the primary antibody.

Statistical analysis for RT-PCR

Experiments were performed with liver tissue slices from eight human donors and 10 mouse donors in triplicates. Real-time PCR results were compared using Student's *t*-test assuming nonequal variance and independence.

Results

Demonstration of productive adenoviral replication in mouse and human liver tissue slice models

Although previous studies have shown poor human adenoviral replication *in vivo* in rodents,[9,10] we compared the extent of adenoviral replication in our *ex vivo* model using human and mouse liver tissue slices (Figure 1). For this, mouse and human liver tissue slices were infected with nonreplicating Adnull [E1−] or replicating AdΔ24 [E1+] at 500 viral particles/cell, a titer consistent with maximum infectivity (data not shown). Following infection, E4 copy number (a surrogate for adenoviral genome copy number) was analyzed at 12 and 28 h by quantitative real-time RT-PCR.[14] In human liver tissue slices, AdΔ24 showed evidence of replication between 12 and 28 h after infection, by an increase in E4 copy number from 750 ± 100 to 2100 ± 500 (a 2.9 ± 0.7-fold increase) (Figure 1a). Mouse liver tissue slices showed a more modest AdΔ24 replication between 12 and 28 h, with the E4 copy number increasing from 130 ± 5 to 175 ± 10 (a 1.36 ± 0.07-fold increase) (Figure 1b). The Adnull E4 copy number remained at low levels in both human and mouse liver slices, consistent with its nonreplicative phenotype (data not shown).

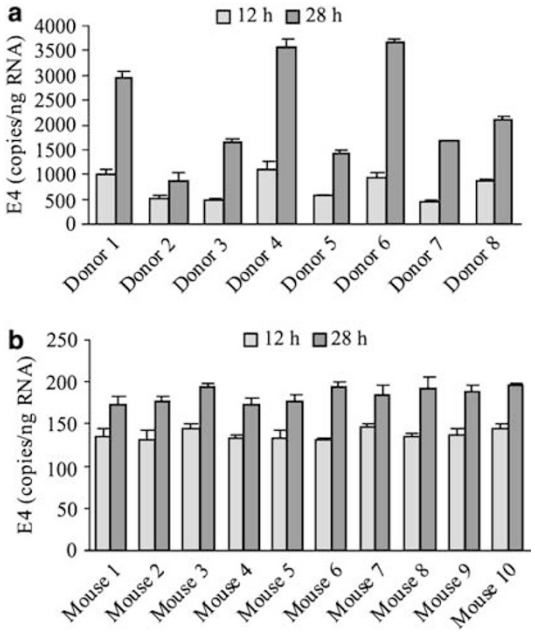

Figure 1 Evaluation of AdΔ24 replication in human (**a**) and mouse (**b**) liver tissue slices. Primary human and mouse liver tissue samples were sliced with the Krumdieck thin-slice tissue slicer and infected in 12-well plates with 500 vp/cell of Adnull [E1−] and AdΔ24 [replication-competent] and evaluated for viral replication at 12 and 28 h by quantitative reverse transcription PCR for adenoviral E4 copy number. Results are displayed in number of copies/ng RNA as determined against GAPDH expression. All data points are triplicates of slices; bars ± s.d.

Comparison of Adnull and AdΔ24 mediated direct hepatotoxicity by determination of extracellular release of liver enzymes

We next examined the correlation between AdΔ24 replication and toxicity in mouse and human liver tissue slices. To accomplish this, we compared the toxicity of Adnull and AdΔ24 in the human and mouse liver tissue slice models by measuring the release of aminotransferase enzymes in the extracellular matrix milieu,[13] which is widely used as a surrogate marker for liver damage. As a sensitive marker of hepatocellular injury, we quantitated ALT, LDH and AST levels at 4, 10, 28, and 43 h postinfection in the culture medium of liver tissue slices from eight human liver samples (Figure 2) and from 10 mouse liver samples (Figure 3). Based on the relatively poor replication of AdΔ24 in mouse liver tissue slices compared to human liver tissue slices demonstrated above, we hypothesized that little or no liver toxicity would be displayed. Surprisingly, in both human and mouse liver tissue slices, infection with AdΔ24 resulted in a statistically significant higher ALT, LDH and AST release ($P < 0.05$) than infection with Adnull between 28 and 43 h post-infection (Figures 2 and 3). These results demonstrate that both mouse and human liver tissue slices infected with AdΔ24 had increased hepatotoxicity compared to noninfected tissue slices or tissue slices infected with the nonreplicative Adnull. However, a correlation

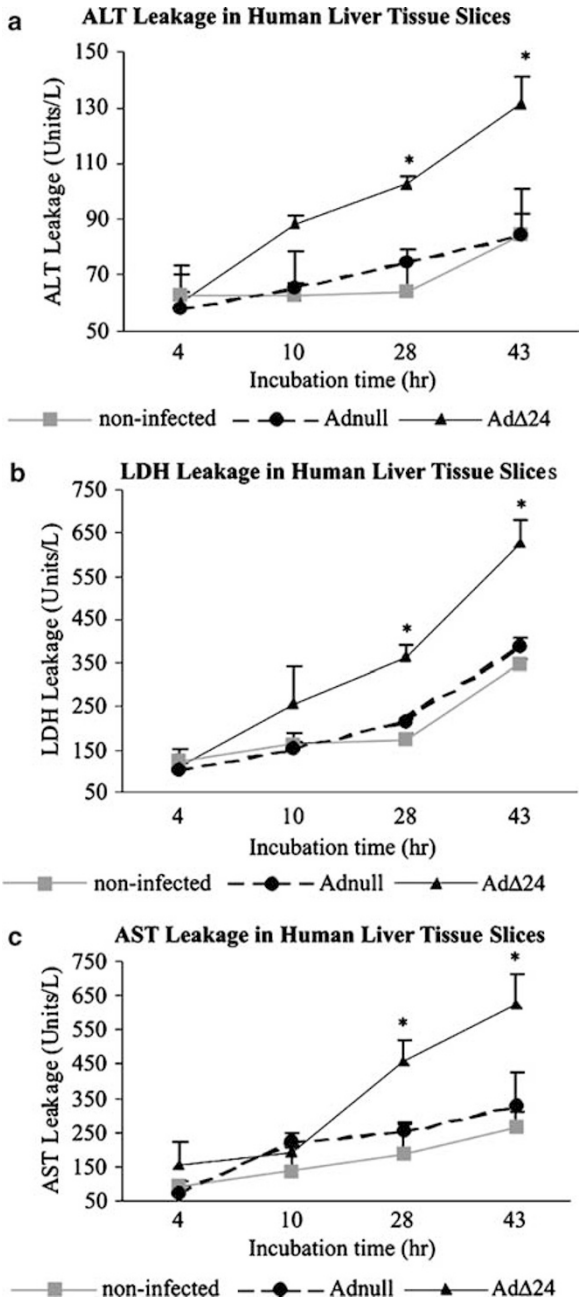

Figure 2 Extracellular release of ALT (**a**), LDH (**b**) and AST (**c**) into the culture medium of human liver tissue slices after different incubation times (in hours). *$P<0.05$ Adnull versus AdΔ24 infected human liver tissue slices. All data points are triplicates of slices; bars $\pm$ s.d.

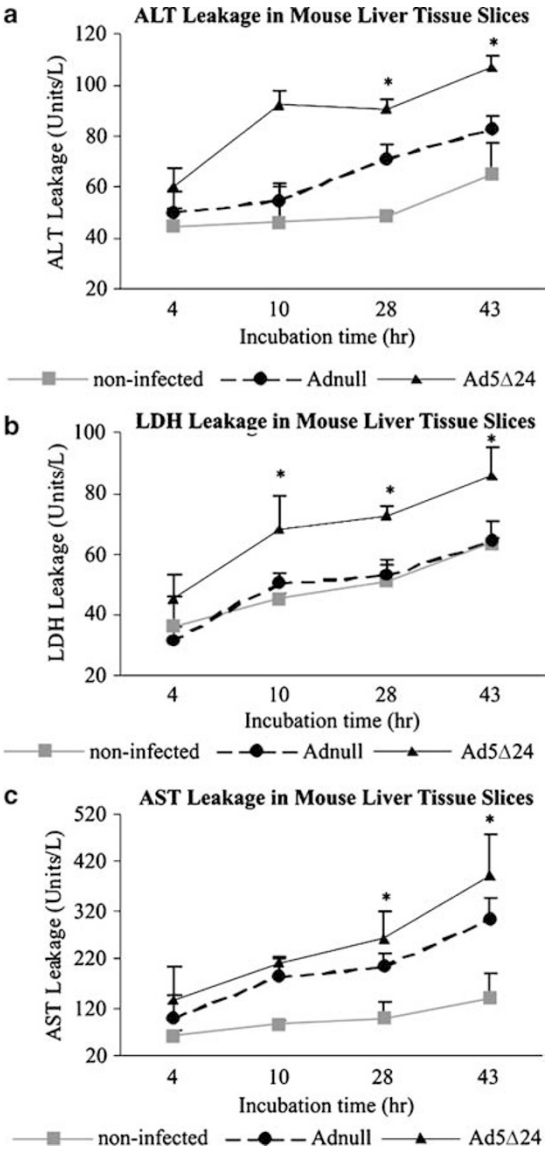

Figure 3 Extracellular release of ALT (**a**), LDH (**b**) and AST (**c**) into the culture medium of mouse liver slices after different incubation times (in hours). *$P<0.05$ Adnull versus AdΔ24 infected mouse liver tissue slices. All data points are triplicates of slices; bars $\pm$ s.d.

between AdΔ24 replication and toxicity in mouse liver tissue slices was not observed.

Apoptosis as an indicator of direct adenoviral mediated hepatotoxicity

Next, we investigated whether apoptosis could be used as an indicator of CRAd-mediated direct liver toxicity. We evaluated this hypothesis by determining levels of caspase-3 activity assessed by immunohistochemical staining of human liver tissue slices (Figure 4). Antibodies directed against an epitope on caspase-3 were immunohistochemically nonreactive in the control human liver tissue slice (Figure 4a) as well as in the Adnull infected human liver tissue slices after 28 h of infection (Figure 4b). However, an immunoreactive (positive) cytoplasmic and nuclear caspase-3 staining was observed in the AdΔ24 infected human liver tissue slices (Figure 4c). These results show that apoptosis was undetectable by caspase-3 immunohistochemical staining in human liver slices infected by nonreplicating Adnull. Importantly, apoptosis was detected in human liver slices infected by the replicating AdΔ24. These results suggest

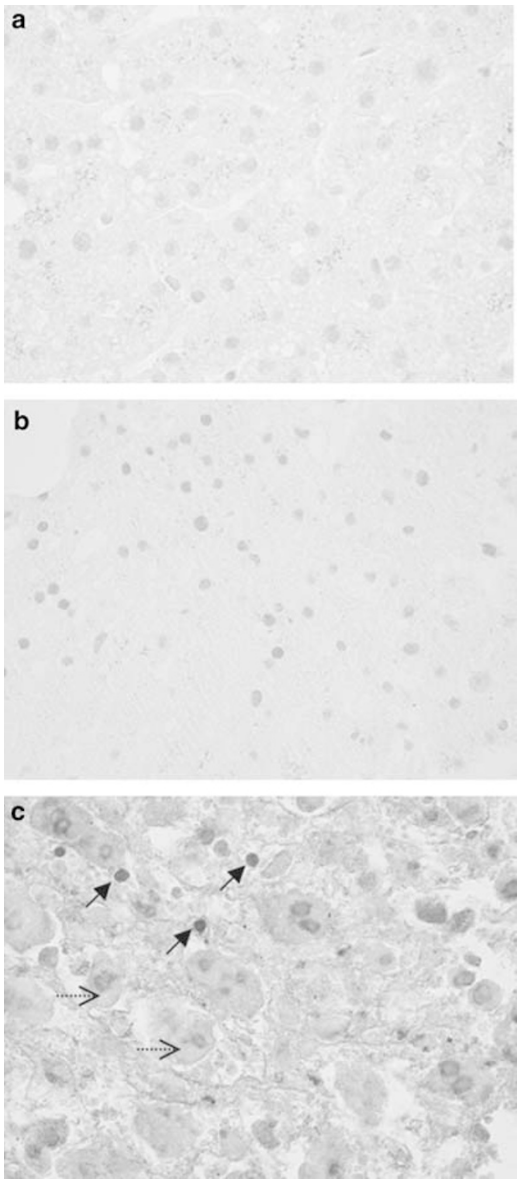

Figure 4 Evaluation of caspase-3 immunhistochemical staining in human liver tissue slices at 28-h time point. Under light microscopy, the control human liver tissue slice (**a**) and the Adnull infected human liver tissue slice (**b**) showed no immunoreactivity for caspase 3. (**c**) Active caspase-3 staining was observed in the nucleus (⟶) and the cytosol (⇢) of hepatocytes in AdΔ24 infected human liver tissue slice.

that apoptosis may be used as a surrogate marker for demonstration of AdΔ24 mediated liver toxicity in the human liver tissue slice model.

Determination of Adnull and AdΔ24 direct mediated hepatotoxicity by TUNEL assay

Next, we investigated whether we could correlate AdΔ24-mediated hepatotoxicity in human liver tissue slices compared to mouse liver tissue slices by detection of DNA fragmentation using TUNEL assays at 28 h after adenoviral infection (Figure 5). In both the mouse and the human liver tissue slices, no TUNEL positive cells were detected either in the noninfected control or in the Adnull infected liver tissue slices (Figure 5a and b). In contrast, positive nuclei (brown nuclei with nuclear condensation) were observed in hepatocytes from the mouse and human liver tissue slices infected with AdΔ24 (Figure 5c). These data that AdΔ24 induced apoptosis is detected by TUMEL assay in the human liver slice model, are consistent with the results of caspase 3 immunohistochemical staining shown in Figure 4. Importantly, AdΔ24 induced apoptosis was detected by TUNEL assay not only in the human but also in the mouse liver tissue slices model.

Comparison between Adnull and AdΔ24 mediated direct liver toxicity by microarray analysis and quantitative real-time reverse transcription RT-PCR

Finally, we profiled and evaluated changes in apoptosis gene expression in mouse and human liver tissue slices after infection with the nonreplicative Adnull or the replicative AdΔ24, using microarray analysis. For this, liver tissue slices from a single human donor and from a single mouse donor were infected with Adnull or with AdΔ24 and compared to their noninfected counterparts. In this experiment, the microarray data served as an indicator of changes in expression of apoptosis genes in mouse and liver tissue slices after Ad infection. Expression was detected in 155 overlapping genes involved in apoptosis that were common to both the human and the mouse liver tissue slices; apoptosis genes showing a two-fold or greater change were considered to be significantly modulated. Of these, 15 (9.7%) were classified as upregulated after infection with AdΔ24 or Adnull, compared to noninfected liver tissue slices (Table 1). In addition, 7 (4.5%) of these were classified as down-regulated (Table 2). Expression was also detected in 150 apoptosis genes that were unique to the human liver tissue slices. Of these, 19 (12.6%) were changed after infection with AdΔ24 or Adnull, compared to noninfected human liver tissue slices Table 3). Finally, expression was detected in 90 apoptosis genes that were unique to the mouse liver tissue slices Of these, 15 (12.6%) were changed after infection with AdΔ24 or Adnull, compared to noninfected mouse liver tissue slices (Table 4).

To quantitatively evaluate and confirm the descriptive analysis of our microarray assay, we selected nine different representative apoptosis genes (Table 1, indicated in bold) common between human and mouse, which showed more than two-fold increase after infection with either Adnull or AdΔ24. The expression levels of these nine genes were analyzed by quantitative real-time RT-PCR in matched Adnull and AdΔ24 infected liver tissue slices from human donors and mice. First, samples derived from Adnull infected human liver tissue slices were compared to samples derived from AdΔ24 infected human liver tissue slices ($n=8$). Next, samples derived from Adnull infected mouse liver tissue slices were compared to samples derived from AdΔ24 infected mouse liver tissue slices ($n=10$). Table 5 represents the results of

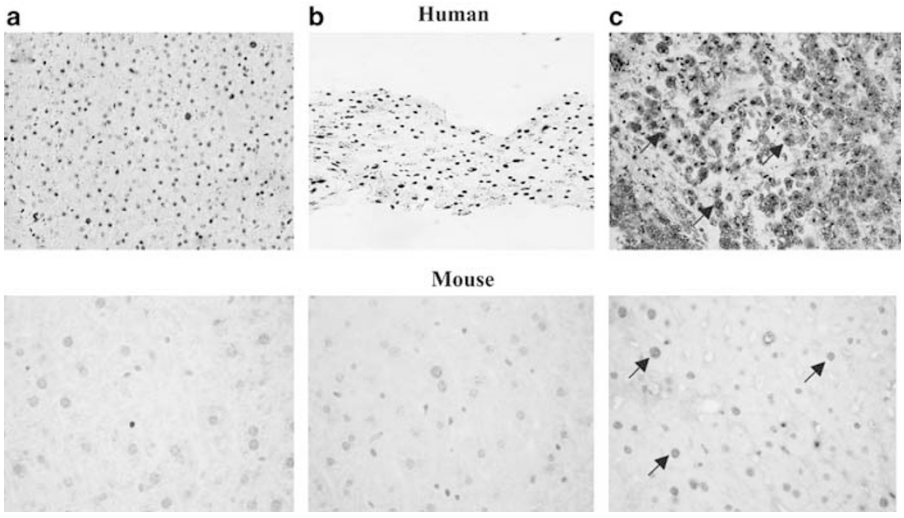

Figure 5 AdΔ24 induces apoptosis in the mouse and the human liver tissue slice model at the 28-h time point as detected by a TUNEL assay. As seen by conventional light microscopy, the control (**a**) and Adnull infected (**b**) mouse and human liver tissue slices showed no immunoreactivity, whereas AdΔ24 infection in the mouse and human liver tissue slices (**c**) led to TUNEL-immunoreactivity in the hepatocytes (⟶ brown nuclear staining).

the quantitative PCR analysis for these selected apoptosis genes, listing the number of individual human or mouse liver donors showing a significant upregulation of apoptosis genes after infection with AdΔ24 compared to Adnull for each gene. Next, we compared the average expression of apoptosis genes among all Adnull infected human liver tissue slices compared to all AdΔ24 infected human liver tissue slices for each donor. The same analysis was performed for the Adnull and AdΔ24 infected mouse liver tissue slices for each donor. In this regard, the analysis of quantitative real-time PCR results showed a significantly ($P<0.05$) different expression in eight out of nine selected apoptosis genes (Table 5, symbol indicated in bold). For each of these eight apoptosis genes, at least 30% of the human liver donors and 70% of the mouse liver donors were shown to have a significantly higher upregulation by AdΔ24 when compared to Adnull. These results thus confirm the increased apoptosis induction by AdΔ24 infection compared to Adnull in both tissue slice models, as observed in the other toxicity assays performed in this study.

Discussion

Useful models to evaluate potential liver toxicity of adenoviral gene therapies, particularly adenoviral virotherapy, are urgently required. Whereas virotherapy has emerged as a novel and promising approach for neoplastic diseases such as ovarian cancer, the limited repertoire of appropriate model systems has hampered clinical translation of candidate conditionally replicative adenovirus agents (CRAds). To address this issue, we have explored the method to derive tissue explants from human and normal tissues via a tissue slice technique using the Krumdieck tissue slicer.[14] We showed the fidelity of adenovirus replication between known *in vitro* cell lines and their related tissue slice explants.[14] Finally, and most importantly, we established the utility of tissue slices for monitoring adenovirus replication in primary human tumors as well as replication selectivity using human liver.[14] On this basis, we have extended our studies herein to investigate whether our novel human liver tissue slice model could provide a mean to more fully characterize CRAd-mediated liver toxicity.

First, we investigated whether the observed liver toxicity in the human liver tissue slice model was related to the replicative phenotype of the conditionally replicative adenovirus AdΔ24, currently in phase I trials.[22] In this regard, AdΔ24 contains a 24-bp deletion in the CR2 of the E1A gene,[18,19] and serves as a representative CRAd to determine differences in liver toxicity compared to a representative nonreplicating adenovirus (Adnull). Since human serotype adenoviruses developed as CRAds undergo only limited replication in a murine host background,[10] we sought to validate this notion by comparing AdΔ24 replication in human and mouse liver tissue slices. Human adenovirus undergoes abortive infection in murine target cells characterized by high early gene expression with early to late transition blocks.[9] Based on this consideration, the low E4 copy number in murine liver and the three-fold higher copy number in human liver was not unexpected.

Next, we sought to compare the AdΔ24 and Adnull induced toxicity between the human and the mouse liver tissue slice model. In this regard, extracellular release of the aminotransferases ALT, LDH and AST were significantly higher after infection with AdΔ24 than Adnull in both human and mouse liver tissue slices. These findings question the original hypothesis relating viral replication in the S-phase of the cell cycle to

Table 1 Descriptive microarray results of apoptosis genes common to human and mouse liver tissue slices that were upregulated after infection with Adnull or AdΔ24

Human	*Mouse*			*Human*		*Mouse*	
Gene bank accession number	*Gene bank accession number*	*Gene name*	*Symbol*	*Fold change (Adnull)*	*Fold change (Ad5Δ24)*	*Fold change (Adnull)*	*Fold change (Ad5Δ24)*
AI378406	BB284358	egl nine homolog 3 (*C. elegans*)	**EGLN3**	5.81	12.9	5.8	11
AF060922	AK018668	BCL2/adenovirus E1B 19 kDa interacting protein 3-like	**BNIP3L**	3.24	4.4	NC	2.09
BC015944	BG518542	TIA 1 cytotoxic granule-associated RNA binding protein	**TIA1**	3.03	3.53	2.3	3.97
NM_001775	BB256012	CD38 antigen (p45)	**CD38**	2.12	2.98	NC	2.49
AF078077	AK010420	Growth arrest and DNA-damage-in inducible, beta	**GADD45B**	2.14	2.83	49.18	67.98
BF224259	BG071121	Survival motor neuron domain containing 1	SMNDC1	NC	2.04	2.41	2.6
M13436	NM_008380	Inhibin, beta A (activin A, activin AB alpha polypeptide)	INHBA	2.2	2.9	10	10.6
U19599	BC018228	BCL2-associated X protein	**BAX**	2	2.86	4.5	5.5
NM_002583	BB398886	PRKC, apoptosis, WT1, regulator	PAWR	2.26	2.8	3.9	4.9
AI990766	AW557263	Fragile X mental retardation, autosomal homolog 1	FXR1	3.13	2.69	2.46	NC
AF082283	AF100339	B-cell CLL/lymphoma 10	**BCL10**	2.51	2.49	2.82	4.43
NM_004346	BG070529	Caspase 3, apoptosis-related cysteine protease	**CASP3**	2	3.03	2.28	3.23
U25804	NM_007609	Capase 4, apoptosis-related cysteine protease	**CASP4**	2.3	2.43	5.65	5.89
NM_015322	BM232562	Fem-1 homolog b (*C. elegans*)	FEM1B	2.1	NC	4.5	3.5
NM_013374	C76364	Programmed cell death 6 interacting protein	PDCD6IP	2.04	2.2	2.4	2.46

Only genes with $\geqslant$2-fold change were considered to be modulated.
NC = no change.

Table 2 Descriptive microarray results of apoptosis genes common to human and mouse liver tissue slices that were downregulated after infection with Adnull or AdΔ24

Human	*Mouse*	*Gene name*	*Symbol*	*Human*		*Mouse*	
Gene bank accession number	*Gene bank accession number*			*Fold change (Adnull)*	*Fold change (Ad5Δ24)*	*Fold change (Adnull)*	*Fold change (Ad5Δ24)*
NM_014456	NM_011050	Programmed cell death 4 (neoplastic transformation inhibitor)	PDCD4	NC	2.09	−5.4	−4.59
AF119841	NM_023523	Peroxisomal trans 2-enoyl CoA reductase	PECR	−2.1	−2.08	−12.2	−7.6
BF508639	NM_019423	Catenin (cadherin-associated protein), alpha-like 1	CTNNAL1	−3	−2.3	−6.36	−4.1
AF131850	NM_007915	Etoposide induced 2.4mRNA	EI24	−2.3	−2.43	−2.6	−2.7
AB033078	NM_009163	Sphingosine-1-phosphate lyase 1	SGPL1	NC	−2.07	2.28	2.69
NM_005256	NM_008087	Growth arrest-specific 2	GAS2	−6.19	−5.54	−4	−2.01
AD00092	NM_010062	Deoxyribonuclease II, lysosomal	DNASE2	−2.8	NC	−9.5	−4.25

Only genes with ⩾2-fold change were considered to be modulated.
NC = no change.

Table 3 Descriptive microarray results of apoptosis genes unique to human liver tissue slices that were up- or downregulated after infection with Adnull or AdΔ24

Gene bank accession number	*Gene name*	*Symbol*	*Fold change (Adnull)*	*Fold change (Ad5Δ24)*
AF511652	Caspase recruitment domain family, member 8	CARD8	3.36	3.81
NM_005894	CD5 antigen-like (scavenger receptor cysteine-rich family)	CD5L	2.25	2.85
AF348491	Chemokine (C-X-C motif) receptor 4/// chemokine (C-X-C motif) receptor 4	CXCR4	8.75	10.7
BF686824	Death-associated protein kinase 3	DAPK3	3.2	3.29
NM_003824	Fas (TNFRSF6)-associated via death domain	FADD	2.51	2.69
BC005352	TNF-induced protein	GG2-1	7.01	7.57
NM_002656	Pleiomorphic adenoma gene-like1	PLAGL	2.64	2.41
NM_006663	RelA-associated inhibitor	RAI	2.43	3.18
NM_004760	Serine/threonine kinase 17a (apoptosis-inducing)	STK17A	2.77	3.46
NM_003844	Tumor necrosis factor receptor superfamily, member 10a	TNFRSF 10A	281	4.56
AF021233	Tumor necrosis factor receptor superfamily, member l0d, decoy with truncated death domain	TNFRSF 10D	7.21	7.94
AI084226	Regulator of Fas-induced apoptosis	TOSO	14.93	17.03
NM_005426	Tumor protein p53 binding protein, 2	TP53BP	2.3	2.39
NM_004619	TNF receptor-associated factor 5	TRAF5	7.11	4.96
NM_002507	Nerve growth factor receptor (TNFR superfamily, member 16)	NGFR	−16.22	−14.72
D32201	Adrenergic, alpha-lA-, receptor	ADRA1	−4.32	−5.46
BF448201	Cullin 5	CUL5	−2.33	−2.93
A1760495	Cytochrome *c*, somatic	CYCS	−2.33	−2.77
NM_006705	Growth arrest and DNA-damage-inducible, gamma	GADD4	−2.41	−2.55

Only genes with ⩾2-fold change were considered to be modulated.

toxicity.[23] The observed AdΔ24 mediated hepatotoxicity in the mouse liver tissue slices suggests that the effects of various E1A-mutants on S-phase induction, viral replication, and cytotoxicity may not be directly related. The mechanisms of reduced cytotoxicity of AdΔ24 in normal cells thus remain unclear.[23]

In addition, we sought to compare AdΔ24 and Adnull mediated liver toxicity in human liver by using apoptosis as an indicator. Previous studies of apoptosis in viral hepatitis applied a variety of different methods, including activation of caspase-3[24–26] and TUNEL assays[27,28] as surrogate markers. Our results demonstrate that positive caspase-3 immunoreactivity was indeed observed in human liver tissue slices infected with AdΔ24, but not Adnull. In addition, both human and mouse liver tissue slices showed positive TUNEL staining when infected with AdΔ24 but not with Adnull. Importantly, these data agree with the higher extracellular release of

Table 4 Descriptive microarray results of apoptosis genes unique to mouse liver tissue slices that were up- or downregulated after infection with Adnull or AdΔ24

Gene bank accession number	*Gene name*	*Symbol*	*Fold change (Adnull)*	*Fold change (Ad5Δ24)*
BC025541	Bcl2-like 14 (apoptosis facilitator)	Bcl2114	7.73	13.45
NM_007610	Caspase 2	Casp2	2.93	2.89
BC011437	Interleukin 1 beta	Illb	1.51	1.99
NM_011577	Transforming growth factor, beta 1	Tgfb1	4.44	5.28
NM_013749	Tumor necrosis factor receptor superfamily, member 12a	Tnfrsf1	29.04	35.51
NM_024290	Tumor necrosis factor receptor superfamily, member 23	Tnfrsf2	10.34	26.17
NM_009404	Tumor necrosis factor (ligand) superfamily, member 9	Tnfsf9	26.35	58.89
NM_011632	Tnf receptor-associated factor 3	Traf3	7.21	5.28
AJ297973	Transformation related protein 53	Trp53	3.97	5.94
NM_009811	Caspase 6	Casp6	−4.56	−2.33
U67321	Caspase 7	Casp7	−6.28	−2.31
NM_009894	Cell death-inducing DNA fragmentation factor, alpha subunit-	Cideb	−7.11	−5.03
AJ224740	CASP and RIPK domain containing adaptor with death	Cradd	−2.45	−2.13
BM248206	Growth arrest specific 2	Gas2	−3.97	−3.94
NM_008360	Interleukin 18	Il18	−6.77	−5.46

Only genes with ⩾2-fold change were considered as modulated.

Table 5 Validation of representative apoptosis genes in the descriptive microarray hybridization by quantitative real-time RT-PCR to compare apoptosis gene expression in human liver tissue slices after infection with Adnull and AdΔ24 to noninfected human liver tissue slices

Gene bank accession number	*Gene bank accession number*	*Gene name*	*Symbol*	*No. of patients showing a significant higher upgredation of apoptosis genes after infection with AdΔ24 compared to Adnull*	*No of mice showing a significant higher upregulation of apoptosis genes after infection with AdΔ24 compared to Adnull*
AI378406	BB284358	egl nine homolog 3 (*C. elegans*)	**EGLN3**	6/8 (75%)	9/10 (90%)
AF060922	AK018668	BCL2/adenovirus E1B 19 kDa interacting protein 3-like	**BNIP3L**	5/8 (62%)	7/10 (70%)
BC015944	BG518542	TIA1 cytotoxic granule-associated RNA binding protein	**TIA1**	3/8 (40%)	7/10 (70%)
NM_001775	BB256012	CD38 antigen (p45)	**CD38**	2/8 (25%)	8/10 (80%)
AF078077	AK010420	Growth arrest and DNA-damage-inducible, beta	**GADD45B**	3/8 (40%)	10/10 (100%)
U19599	BC018228	BCL2-associated X protein	**BAX**	3/8 (40%)	8/10 (80%)
AF082283	AF100339	B-cell CLL/lymphoma 10	**BCL10**	4/8 (50%)	8/10 (80%)
NM_004346	BG070529	Caspase 3, apoptosis-related cysteine protease	**CASP3**	4/8 (50%)	7/10 (70%)
U25804	NM_007609	Capase 4, apoptosis-related cysteine protease	CASP4	1/8 (12.5%)	0/10 (0%)

The number of donors and mice showing a significant upregulation of the selected apoptosis genes in liver tissue slices after infection with AdΔ24 compared to Adnull are indicated. All data points are triplicates of slices.

aminotransferase enzymes in liver slices infected with AdΔ24 compared to Adnull.

Finally, we investigated the effects of Adnull and AdΔ24 infection on apoptosis gene expression via microarray analysis. We identified 15 apoptosis genes common to both human and mouse liver tissue slices that were upregulated and seven apoptosis genes that were downregulated after Ad infection of liver slices. Nine of these upregulated apoptosis genes were selected for verification by real-time RT-PCR. Of note, the evaluation of apoptosis gene expression occurred at 28 h after adenoviral infection, based on our previous data, which indicated that this time point was optimal for evaluation and viability of Ad infected tissue slices.[14] The apoptosis genes chosen included EGLN3, BNIPL3L, TIA-1, CD38 (p45), GADD45b, BAX, BCL10, CASP3 and CASP4.

Our RT-PCR data verified a statistically significant upregulation of caspase-3 in the AdΔ24 infected human

and mouse liver tissue slices, as also observed in our immunohistochemical analysis. Of the 11 capsases identified to date, caspase-3 is considered a central player mediating apoptosis, correlating this result with the observed TUNEL staining in AdΔ24 infected liver slices. Other regulators of apoptosis include the Bcl-2 family.[29,30] In this regard, the observed upregulation of both Bax and BNIPL-3 in human and mouse liver tissue slices after AdΔ24 infection also corresponds to the observed increase in apoptosis.

In addition to proteins of the Bcl-2 family, EGLN3, a homologue of the *Caenorhabditis elegans* gene egl-9[31] was increased by AdΔ24 in human and mouse liver tissue slices. EGLN3 has been implicated in the regulation of growth, differentiation and apoptosis in muscle and nerve cells. Furthermore, the proapoptotic proteins Bcl10, TIA-1[32] and GADD45b[33] were strongly induced in AdΔ24 infected human and mouse liver tissue slices, corroborating the induction of apoptosis on AdΔ24 infection.

In our study AdΔ24, which contains a 24-bp deletion in the CR2 of the E1A gene,[18,19] served as a representative CRAd to determine differences in liver toxicity compared to Adnull. In this regard, the effects of E1A on cellular biology are extremely complex and poorly understood. The adenoviral E1A gene product plays a critical role in altering the biology of resting normal cells to facilitate viral replication. Modification of the adenoviral E1A gene is an attractive way to restrict viral replication to proliferating cells.[23] Wild-type E1A binds to Rb, thereby releasing E2F and inducing S phase, a process that is thought to be important for viral replication in resting cells. AdΔ24 containing a deletion of the Rb-binding site within E1A has been hypothesized to be defective in inducing S phase and therefore replication-impaired in normal cells, while retaining full replication capacity in cells with defective Rb function.[18,19]

The Rb pathway is inactive in almost all human tumors, including ovarian cancer.[18,19] However, our results indicate that a deletion of the Rb-binding site in E1A alone does not prevent hepatotoxicity. In this context, it has been shown that deletion of the Rb-binding site in E1A alone has only a small effect on the ability of the virus to induce S phase.[23] AdΔ24 can replicate to wild-type levels in growth arrested HUVEC[23] and in an organotypic model of human stratified epithelium.[34] In this regard, it has been shown that in addition to deletion of the Rb-binding domain, a deletion within the N-terminus of E1A is required to substantially reduce the ability of the virus to induce S-phase.[23,35,36] It remains unclear which of several E1A modifications that disturb the interaction with various cellular proteins would be most effective at protecting normal cells, while preserving the oncolytic potency of the virus.

Although in this study liver toxicity and apoptosis induction has been demonstrated using our liver tissue slice model, it is important to note that the immune response to adenoviruses is obviously not applicable herein. In this regard, using immune competent animals, most of the administered adenovirus is sequestered and cleared by Kupffer cells.[37] Fulminant hepatotoxicities caused by adenoviruses have been observed in severe immune suppressed patients.[38] Of note, the cotton rat model has been proposed as an animal model to evaluate oncolytic Ad vectors,[39] due to the semipermissive nature of the cotton rat for human Ad replication. Adenovirus biodistribution and replication, as well as any associated organ toxicities have been assessed using E1A-deficient vectors in the cotton rat.[40] To date, the cotton rat model has also been a particularly useful animal model of adenovirus pneumonia.[41,42] While the tissue slice model does not consider the immune response, demonstration of reduced liver toxicity will likely be predictive of an increased therapeutic index. However, to validate this hypothesis, a direct comparison between the determination of adenoviral vector mediated toxicity using tissue slice model and the determination of *in vivo* toxicity on adenovirus administration in the cotton rat model would likely be useful.

In conclusion, useful models for evaluation of *in vivo* liver toxicity of new generation gene therapy vectors are needed. In this regard, the human liver tissue slice model demonstrates CRAd-mediated hepatotoxicity in primary human liver samples with maintained liver structure and composition. Furthermore, a concordance of CRAd mediated liver toxicity in both the human and the mouse liver tissue slice models was demonstrated, despite the reported limited replication ability of CRAds in mice. Thus, our data implicate that the mouse liver tissue slice model may be in fact better than expected in predicting liver toxicity to CRAds. The data presented here thus suggest both liver tissue slice models, human and mouse, to be a valid powerful tool for *ex vivo* preclinical evaluation for virotherapy liver toxicity, to aid in the clinical translation of CRAds.

Acknowledgements

This work was supported by Grant of the Deutsche Forschungsgemeinschaft Sto 647/1-1 (to MA Stoff-Khalili), NIH Grant R01-DK063615 (to M Yamamoto), NIH Grant RO1CA93796 (to GP Siegal), NIH Grants RO1-CA083821, RO1-CA94084, RO1-CA93796 and Mesothelioma grant (to DT Curiel). We thank Minghui Wang and Cecil R Stockard for invaluable technical assistance.

References

1 Nettelbeck DM, Curiel DT. Tumor-busting viruses. *Sci Am* 2003; **289**: 68–75.
2 Nettelbeck DM. Virotherapeutics: conditionally replicative adenoviruses for viral oncolysis. *Anticancer Drugs* 2003; **14**: 577–584.
3 Alemany R, Suzuki K, Curiel DT. Blood clearance rates of adenovirus type 5 in mice. *J Gen Virol* 2000; **81**: 2605–2609.
4 Bernt KM, Ni S, Gaggar A, Li ZY, Shayakhmetov DM, Lieber A. The effect of sequestration by nontarget tissues on anti-tumor efficacy of systemically applied, conditionally replicating adenovirus vectors. *Mol Ther* 2003; **8**: 746–755.

5 Zaiss AK, Liu Q, Bowen GP, Wong NC, Bartlett JS, Muruve DA. Differential activation of innate immune responses by adenovirus and adeno-associated virus vectors. *J Virol* 2002; **76**: 4580–4590.
6 Lieber A, He CY, Meuse L, Schowalter D, Kirillova I, Winther B *et al*. The role of Kupffer cell activation and viral gene expression in early liver toxicity after infusion of recombinant adenovirus vectors. *J Virol* 1997; **71**: 8798–8807.
7 Varnavski AN, Calcedo R, Bove M, Gao G, Wilson JM. Evaluation of toxicity from high-dose systemic administration of recombinant adenovirus vector in vector-naive and pre-immunized mice. *Gene Ther* 2005; **12**: 427–436.
8 Malkinson AM. Molecular comparison of human and mouse pulmonary adenocarcinomas. *Exp Lung Res* 1998; **24**: 541–555.
9 Duncan SJ, Gordon FC, Gregory DW, McPhie JL, Postlethwaite R, White R *et al*. Infection of mouse liver by human adenovirus type 5. *J Gen Virol* 1978; **40**: 45–61.
10 Paielli DL, Wing MS, Rogulski KR, Gilbert JD, Kolozsvary A, Kim JH *et al*. Evaluation of the biodistribution, persistence, toxicity, and potential of germ-line transmission of a replication-competent human adenovirus following intraprostatic administration in the mouse. *Mol Ther* 2000; **1**: 263–274.
11 Boess F, Kamber M, Romer S, Gasser R, Muller D, Albertini S *et al*. Gene expression in two hepatic cell lines, cultured primary hepatocytes, and liver slices compared to the *in vivo* liver gene expression in rats: possible implications for toxicogenomics use of in vitro systems. *Toxicol Sci* 2003; **73**: 386–402.
12 Olinga P, Merema M, Slooff MJ, Meijer DK, Groothuis GM. Influence of 48 h of cold storage in University of Wisconsin organ preservation solution on metabolic capacity of rat hepatocytes. *J Hepatol* 1997; **27**: 738–743.
13 Olinga P, Groen K, Hof IH, De Kanter R, Koster HJ, Leeman WR *et al*. Comparison of five incubation systems for rat liver slices using functional and viability parameters. *J Pharmacol Toxicol Methods* 1997; **38**: 59–69.
14 Kirby TO, Rivera A, Rein D, Wang M, Ulasov I, Breidenbach M *et al*. A novel ex vivo model system for evaluation of conditionally replicative adenoviruses therapeutic efficacy and toxicity. *Clin Cancer Res* 2004; **10**: 8697–8703.
15 Rao XM, Tseng MT, Zheng X, Dong Y, Jamshidi-Parsian A, Thompson TC *et al*. E1A-induced apoptosis does not prevent replication of adenoviruses with deletion of E1b in majority of infected cancer cells. *Cancer Gene Ther* 2004; **11**: 585–593.
16 Duque PM, Alonso C, Sanchez-Prieto R, Lleonart M, Martinez C, de Buitrago GG *et al*. Adenovirus lacking the 19-kDa and 55-kDa E1B genes exerts a marked cytotoxic effect in human malignant cells. *Cancer Gene Ther* 1999; **6**: 554–563.
17 Reed JC, Doctor K, Rojas A, Zapata JM, Stehlik C, Fiorentino L *et al*. Comparative analysis of apoptosis and inflammation genes of mice and humans. *Genome Res* 2003; **13**: 1376–1388.
18 Fueyo J, Gomez-Manzano C, Alemany R, Lee PS, McDonnell TJ, Mitlianga P *et al*. A mutant oncolytic adenovirus targeting the Rb pathway produces anti-glioma effect in vivo. *Oncogene* 2000; **19**: 2–12.
19 Heise C, Hermiston T, Johnson L, Brooks G, Sampson-Johannes A, Williams A *et al*. An adenovirus E1A mutant that demonstrates potent and selective systemic anti-tumoral efficacy. *Nat Med* 2000; **6**: 1134–1139.
20 Krumdieck C. A new instrument for the rapid preparation of tissue slices. *Anal Biochem* 1980; **104**: 118–123.
21 Rivera AA, Wang M, Suzuki K, Uil TG, Krasnykh V, Curiel DT *et al*. Mode of transgene expression after fusion to early or late viral genes of a conditionally replicating adenovirus via an optimized internal ribosome entry site *in vitro* and *in vivo*. *Virology* 2004; **320**: 121–134.
22 Vecil GG, Lang FF. Clinical trials of adenoviruses in brain tumors: a review of Ad-p53 and oncolytic adenoviruses. *J Neurooncol* 2003; **65**: 237–246.
23 Sauthoff H, Pipiya T, Heitner S, Chen S, Bleck B, Reibman J *et al*. Impact of E1a modifications on tumor-selective adenoviral replication and toxicity. *Mol Ther* 2004; **10**: 749–757.
24 Bantel H, Schulze-Osthoff K. Apoptosis in hepatitis C virus infection. *Cell Death Differ* 2003; **10**(Suppl 1): S48–S58.
25 Bantel H, Lugering A, Heidemann J, Volkmann X, Poremba C, Strassburg CP *et al*. Detection of apoptotic caspase activation in sera from patients with chronic HCV infection is associated with fibrotic liver injury. *Hepatology* 2004; **40**: 1078–1087.
26 McPartland JL, Guzail MA, Kendall CH, Pringle JH. Apoptosis in chronic viral hepatitis parallels histological activity: an immunohistochemical investigation using anti-activated caspase-3 and M30 cytodeath antibody. *Int J Exp Pathol* 2005; **86**: 19–24.
27 Papakyriakou P, Tzardi M, Valatas V, Kanavaros P, Karydi E, Notas G *et al*. Apoptosis and apoptosis related proteins in chronic viral liver disease. *Apoptosis* 2002; **7**: 133–141.
28 Rodrigues CM, Brites D, Serejo F, Costa A, Ramalho F, De Moura MC. Apoptotic cell death does not parallel other indicators of liver damage in chronic hepatitis C patients. *J Viral Hepat* 2000; **7**: 175–183.
29 Green DR, Reed JC. Mitochondria and apoptosis. *Science* 1998; **281**: 1309–1312.
30 Kroemer G, Reed JC. Mitochondrial control of cell death. *Nat Med* 2000; **6**: 513–519.
31 Trent C, Tsuing N, Horvitz HR. Egg-laying defective mutants of the nematode *Caenorhabditis elegans*. *Genetics* 1983; **104**: 619–647.
32 Forch P, Valcarcel J. Molecular mechanisms of gene expression regulation by the apoptosis-promoting protein TIA-1. *Apoptosis* 2001; **6**: 463–468.
33 Yoo J, Ghiassi M, Jirmanova L, Balliet AG, Hoffman B, Fornace Jr AJ *et al*. Transforming growth factor-beta-induced apoptosis is mediated by Smad-dependent expression of GADD45b through p38 activation. *J Biol Chem* 2003; **278**: 43001–43007.
34 Balague C, Noya F, Alemany R, Chow LT, Curiel DT. Human papillomavirus E6E7-mediated adenovirus cell killing: selectivity of mutant adenovirus replication in organotypic cultures of human keratinocytes. *J Virol* 2001; **75**: 7602–7611.
35 Howe JA, Mymryk JS, Egan C, Branton PE, Bayley ST. Retinoblastoma growth suppressor and a 300-kDa protein appear to regulate cellular DNA synthesis. *Proc Natl Acad Sci USA* 1990; **87**: 5883–5887.
36 Wang HG, Rikitake Y, Carter MC, Yaciuk P, Abraham SE, Zerler B *et al*. Identification of specific adenovirus E1A N-terminal residues critical to the binding of cellular proteins and to the control of cell growth. *J Virol* 1993; **67**: 476–488.
37 Shayakhmetov DM, Li ZY, Ni S, Lieber A. Analysis of adenovirus sequestration in the liver, transduction of hepatic cells, and innate toxicity after injection of fiber-modified vectors. *J Virol* 2004; **78**: 5368–5381.

38 Wang WH, Wang HL. Fulminant adenovirus hepatitis following bone marrow transplantation. A case report and brief review of the literature. *Arch Pathol Lab Med* 2003; **127**: e246–248.
39 Toth K, Spencer JF, Tollefson AE, Kuppuswamy M, Doronin K, Lichtenstein DL *et al*. Cotton rat tumor model for the evaluation of oncolytic adenoviruses. *Hum Gene Ther* 2005; **16**: 139–146.
40 Rojas-Martinez A, Wyde PR, Montgomery CA, Chen SH, Woo SL, Aguilar-Cordova E. Distribution, persistency, toxicity, and lack of replication of an E1A-deficient adenoviral vector after intracardiac delivery in the cotton rat. *Cancer Gene Ther* 1998; **5**: 365–370.
41 Ginsberg HS, Lundholm-Beauchamp U, Horswood RL, Pernis B, Wold WS, Chanock RM *et al*. Role of early region 3 (E3) in pathogenesis of adenovirus disease. *Proc Natl Acad Sci USA* 1989; **86**: 3823–3827.
42 Pacini DL, Dubovi EJ, Clyde Jr WA. A new animal model for human respiratory tract disease due to adenovirus. *J Infect Dis* 1984; **150**: 92–97.